MRS Communications (2023) 13:350–356

https://doi.org/10.1557/s43579-023-00353-2

MRS Communications

Research Letter

Positron lifetime investigation of Ni–W and Cu–Cr–Zr alloys after severe plastic deformation and annealing

Saad Mesbah, and Khadidja Abib, Faculty of Physics, University of Sciences and Technology Houari Boumediene, El-Alia, BP 32, 16111 Algiers, Algeria
Abderrahim Guittoum, Nuclear Research Centre of Algiers, 2 Bd, Frantz Fanon, BP 399, Alger, Algeria
Mohamed Akou, Imene Bibimoune, and Djamel Bradai, Faculty of Physics, University of Sciences and Technology Houari Boumediene, El-Alia, BP 32, 16111 Algiers, Algeria

Address all correspondence to Djamel Bradai at **bradai_usthb@yahoo.com**

(Received 28 July 2022; accepted 3 March 2023; published online: 16 March 2023)

Abstract

Positron annihilation lifetime spectroscopy was used to investigate the microstructure of commercial Cu–Cr–Zr and Ni–W ultrafine-grained alloys processed by severe plastic deformation namely equal channel angular pressing, accumulative roll bonding and groove pressing and annealing at 600, 900 and 1000°C. All the lifetime spectra bear the same trends and were a sum of three exponential decay components. The dominant vacancy/dislocations component lifetime changed considerably and dropped after high temperature annealing. Positron lifetime spectroscopy results correlated well with microhardness measurements. The results suggest the presence of three stages in Cu–Cr–Zr and Ni–W industrial alloys which were attributed to dislocations storage through severe plastic deformation, recovery-recrystallization and grain growth.

Introduction

Ni–5at.%W (14 wt%) alloy has attracted academic and industrial interests owing to its potential application as Rolling Assisted Biaxially Textured Substrate (RABITS™) for the profitable production of long lengths of high temperature superconducting tapes (HTS).[1] Among the crucial properties of such material are thermal stability, unique crystallographic Cube texture, low lattice misfit, mechanical strength and finally costs. This alloy exhibits good metallurgical and physical properties after Cube {001}<100> texture forming during heavy plastic deformation and subsequent annealing.[2] Cu–Cr–Zr alloys have attracted growing interests in electric/microelectronics areas and nuclear fusion reactors.[3] Conventional cold working as well precipitation of Cr and complex Cu–Zr phases do strengthen these alloys.[3–7]

The Severe Plastic Deformation (SPD) techniques have known a consecration as the best procedures for producing exceptional bulk ultrafine or nanostructured metals and alloys.[8–10] The most widely used techniques are Equal-Channel Angular Pressing (ECAP), High Pressure Torsion (HPT),[9,11] Accumulative Roll bonding[12,13] and Groove Pressing (GP).[14] Considerable grain refinement and high strengthening can be achieved using these plastic deformation techniques contrarily to metallurgical processes like addition of alloying elements or age-hardening.[13] As long as severe plastic deformation processing was capable of producing strong materials with ultrafine grained structure, these techniques were also applied to Cu–Cr–Zr and Ni–W alloys.[2,6]

Refining microstructure by SPD to an ultrafine or nanometer grains improves mechanical and physical properties of the materials, such as strength, ductility and electrical conductivity. These enhancements originate in the combination of very small grain size below 100 nm and the introduction of great amounts of non-equilibrium defects (dislocations, vacancies, grain boundaries) into the material mostly by means of severe plastic deformation.[15,16] Obviously, defects play a central role in the formation of ultrafine grained or nanostructured metals and alloys and are responsible for their formation. Exhaustive analysis of these defects after SPD processing thus becomes extremely crucial in order to understand and tailor the microstructure.[17] Positron annihilation spectroscopy is a well-known non-destructive technique with a high sensitivity to open-volume defects such as vacancies, dislocations and vacancy clusters.[18]

A non-exhaustive surveying of the literature shows that many investigations were devoted to analyze the ultrafine grained and/or nanocrystalline Cu and Ni and theirs alloys using positron annihilation spectroscopy. These materials were prepared either by severe plastic deformation like HPT,[19–22] ECAP[23,24] or by evaporation/sputtering (E/S),[25] electrodeposition (ED),[26] inert gas condensation (IGC).[27] Yuasa et al.[26] have studied the effects of vacancies on deformation of a nanocrystalline Ni–22W film elaborated by ED and annealing. CuCrZr alloys designated for the use in the international thermonuclear experimental reactor (ITER) have been investigated by positron annihilation technique after several heat treatments, hydrogen implantation and subsequent annealing.[28,29]

However, manifestly, the authors are not aware of any study that explicitly investigates the defects and their evolution after SPD and annealing of industrially important Cu–Cr–Zr and Ni–W alloys. Moreover, it seems highly interesting whether the thermal evolution of the ultra fine-grained structure (UFG)

-determined by PALS and hardness measurements- should be similar in UFG Cu–Cr–Zr and Ni–W alloys. This investigation is of technological interest since both alloys are important commercial alloys and such UFG materials after SPD processing may exhibit more attractive physical (conductivity) and mechanical properties (strength).

In this study, a Positron-Lifetime investigation has been carried out on Cu–Cr–Zr and Ni–W alloys after severe plastic deformation by ECAP, ARB and GP and annealing at temperatures close to recrystallization and grain growth. The analysis evidenced a single and dominant τ_1 defect component associated with positrons trapped at vacancies bound to dislocation and any trace of vacancy cluster or microvoids. A considerable drop of the defect component indicated a rapid grain growth and complete recrystallization. The results are compared and discussed based on the published data.

Experimental procedure

The materials considered in this study are of two types. The first is a commercial Cu–1Cr–0.1Zr (wt%) alloy (Goodfellow, UK). Billets of 10 mm diameter and 60 mm length were then machined for ECAP processing and solution heat-treated for 1 h at 1040°C in a protective inert gas atmosphere followed by a subsequent water quenching. The rods were then processed by ECAP at room temperature up to 4 passes using route B_c (sample rotation of 90° along the longitudinal axis in the same direction after each pass). The full details of the ECAP processing can be found in Refs. 6, 7. The second is a Ni–14W (wt%) alloy (which has been kindly provided by APERAM alloys society, France) in the form of strips of 1 mm thickness. The strips were cut into 35 mm × 20 mm × 1 mm rectangular pieces and then degreased in acetone. The descriptive details of ARB and GP processing can be found in Ref. 2. After ECAP, ARB and GP processing, annealing was carried out up to 600, 900 and 1000°C for 1 h under high vacuum for both alloys (pressure close 10^{-6} Pa). These temperatures correspond to recrystallization (~600°C) and grain growth (900–1000°C).

The PALS measurements were performed at Nuclear Research Centre of Algiers (CRNA) by using a conventional fast–fast coincidence system with NE111 plastic scintillators and XP 2020 photomultipliers. The used positron source consists in a 30 μCi of 22Na source deposited on 25 mm-thick kapton foils. The source was sandwiched between two identical alloy samples in order to ensure that no positrons annihilates outside the sample-source system Typically about 2 10^6 annihilation events were collected in each positron lifetime spectrum with a time resolution of 290 ps.

The microhardness of the Cu–Cr–Zr and Ni–W alloys was measured after each ECAP, ARB or GP cycle using a Shimadzu 2 K facility with a diamond pyramid indenter under a loading charge of 2.94N ($Hv_{0.2}$) and indentation time of 20 s. An average of 10 readings were taken near the middle of the sample to obtain the average microhardness value.

Results and discussions

Figure 1 presents a typical positron life time spectra of the Cu–1Cr–0.1Zr (wt%) alloy after ECAP processing up to $N=4$ passes. Almost all the spectra corresponding to the remnant samples (after ECAP, ARB and GP processing and subsequent annealing) bear the same trends. The spectra were analyzed by Lifetime software MELT4[30] as a sum of three exponential decay components (τ_1, τ_2 and τ_3) with their intensities I_1, I_2 and I_3, respectively.

The MELT program, for Maximum Entropy Lifetime Analysis) is based on the Maximum Entropy principle for regularization and a matricial approach which permits a reconstruction of the intensity spectrum without prior knowledge of the number of lifetime components or their values.[30]

The MELT program was originally used as a pre-analysis tool due to the fact that it makes no assumptions on the number of lifetime components, which give a more general idea about the possible components and thus ensures a better understanding of the defects in the studied materials.

Standard deconvolution of the Gaussian resolution function of the spectrometer source and -background correction were also carried out. Two Gaussian components (220 and 350 ps) were taken into account for the resolution function while the source components were 387 for the NaCl crystallites and kapton foil annihilation and 2172 ps for surface effects, respectively.

These source components were preliminary obtained using LT 10 software. These correction terms were improved in order to get low chi squared values (χ^2 less than 1.15) and then implemented in MELT4 in a special user-defined input file that contains instructions about the subtraction of the source contribution. This was given by the declaration of the Sourcetime and sourceint parameters. Globally, quite close lifetime values were obtained using LT10 for almost all Ni–W

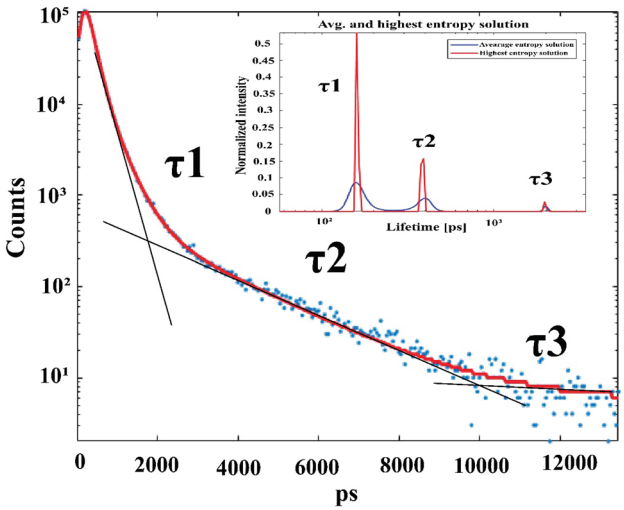

Figure 1. Typical positron life time spectra of the Cu–1Cr–0.1Zr (wt%) alloy after ECAP processing up to $N=4$ passes.

samples with relatively low chi squared values ($\chi^2 \sim 1.186$) but higher values were obtained for Cu–Cr–Zr samples. Comparatively to the literature, MELT4 gave more acceptable lifetime values than LT10.

Figure 1 presents the evolution of the τ_1 lifetime of the Cu–1Cr–0.1Zr (wt%) alloy after ECAP processing and aging and Ni–14W (wt%) alloy after ARB processing up to 2 cycles and GP up to 2 cycles and aging. Table I consigns the evolution of the τ_1 component and its intensity in function of the thermo-mechanical processing. It is worth noting that the source contribution τ_2 and τ_3 values (not shown here) were around 397 ps and 2157 ps with standard deviations close to 17 and 90 ps, respectively. The total contribution of the source was around 31% (30%LT). These values are quite close to those tabulated by Lounis-Mokrani et al.[31] Thereafter, the discussion of the results will be focused on the τ_1 component which represents positron annihilation at defects.

For example, it has been assumed that the reported positron bulk life time for Cu from the tabulated data varies from 103 to 122 ps and the trapped positron lifetime in single vacancy is around 179–182 ps, in dislocations around 170–182 ps and in vacancy clusters from 220 to 350 ps.[32] Therefore very plausibly, τ_1 component should correspond to positrons trapped in single vacancy or in dislocations. A close inspection and comparison of the published data indicates that $\tau_1 \sim 179$ (for $N=0$) with relative intensity of 69% is more likely to be ascribed to the positrons trapped at dislocations than in single vacancies.[33–37] Indeed, Cizek et al.[20] stated that dislocations created during severe plastic deformation represent the dominating type of defects in HPT-deformed Cu samples.

Table I. Evolution of the τ_1 life time with its relative intensities in Cu–Cr–Zr and Ni–W alloys after SPD processing by ECAP, ARB and GP and subsequent aging.

	τ_1 (ps)	I_1 (%)
Cu–Cr–Zr, ECAP		
$N=0$	179.5 190	69.4±0.8
$N=4$	163.9 185	68.2±1.2
$N=4+650°C$	157.8 184	65.4±1.0
$N=4+900°C$	144.5 177	62.6±0.9
Ni–W		
ARB		
$N=0$	169.4 198	65.1±0.8
$N=2$	166.5 183	69.9±0.6
$N=2+600°C$	164.8 179	65.9±0.8
$N=2+1000°C$	142.2 176	63.6±0.5
Ni–W		
GP		
$N=0$	169.4 198	65.1±0.8
$N=2$	165.7 181	68.4±0.6
$N=2+600°C$	167.7 181	70.8±0.6
$N=2+1000°C$	148.5 178	65.2±0.6

A PALS analysis of an HPT processed 99.95% purity Cu evidenced the absence of monovacancies.[19] Very plausibly, the monovacancies created during HPT-processing either disappear by diffusion to sinks such as grain boundaries or agglomerate into small clusters.[19] But this process is valid provided that the grain size is smaller than the positron diffusion length (d_{Cu} ~100 nm, d_{Ni} ~100 nm). This may not be the case in the present study since the grain size of Cu- or Ni-based alloys does never reach such low values even after ECAP, ARB and GP processing. It is worth noting the absence of a positron lifetime which corresponds to the trapping at vacancy clusters or microvoids which are often created due to severe plastic deformation processing.[37] In the case of UFG materials such defects are situated inside grains[10] rather than at triple junction as it was observed in nanocrystalline materials.[38] Indeed, this component value ranged between 252 and 299 ps.[25,36,38] This range is well below the value of τ_2 lifetime that corresponds to the trapping at the crystallite NaCl source and kapton foil.[31,38] In the present work, τ_2 and its intensity I_2 exhibit an almost mean values of 397 ps and 29% with standard deviation of 16 ps and 2.5%, respectively.

After thermo-mechanical processing of Cu–Cr–Zr alloy, the positron lifetime τ_1 shows significant changes [Fig. 2(a)]. It surprisingly decreases from 179.5 ps for the as received state ($N=0$) to 163.9 ps for the ECAP processed one up to 4 passes via route Bc. The intensity of this component decreased very faintly. It can be speculated that this may be explained by a small recovery of the dislocations microstructure. This kind of defects can be recovered more easily than vacancy clusters.[30,31] A quite slower value is seen after annealing at 650°C for 1 h where τ_1 reaches 157.8 ($I_1=65.4\%$) but globally, it can be thought that the defect structure remains stable. Hakatemaya et al.[39] have measured quite close lifetime values in un-deformed Cu–0.78%Cr–0.13%Zr alloy during multi-step aging and re-aging at 460° and 600°. However, their values were given by averaged positron lifetimes between the bulk and vacancy-like defects (vacancies and/or dislocations.

Slugen et al.[28] have evidenced in CuCrZr alloy two main components which first one (~195 ps) indicates changes in the bulk with defects like mono or di-vacancies and the second gives information about large vacancy clusters or voids. The shorter lifetime decreases with increasing positron implantation energy. The intensity of this component approaches 100% with increasing positron energy. The longer component ranges from 400 to 480 ps and corresponds to microvoids and its intensity is very small. In their very recent advanced positron annihilation studies of CuCrZr alloys, Slugen et al.[29] have considered the effect of prior heat treatments on the defect structure in non-irradiated alloys. They identified also two components: τ_1 ascribed to trapping in the bulk and τ_2 which they labeled "defect parameter" and assigned to vacancy-type defect (combination of mono-or di-vacancies with dislocations) in material. However, they assumed the interpretation of the results as not straightforward because the difference between lifetime of mono-, di-vacancies or screw/edge dislocation are

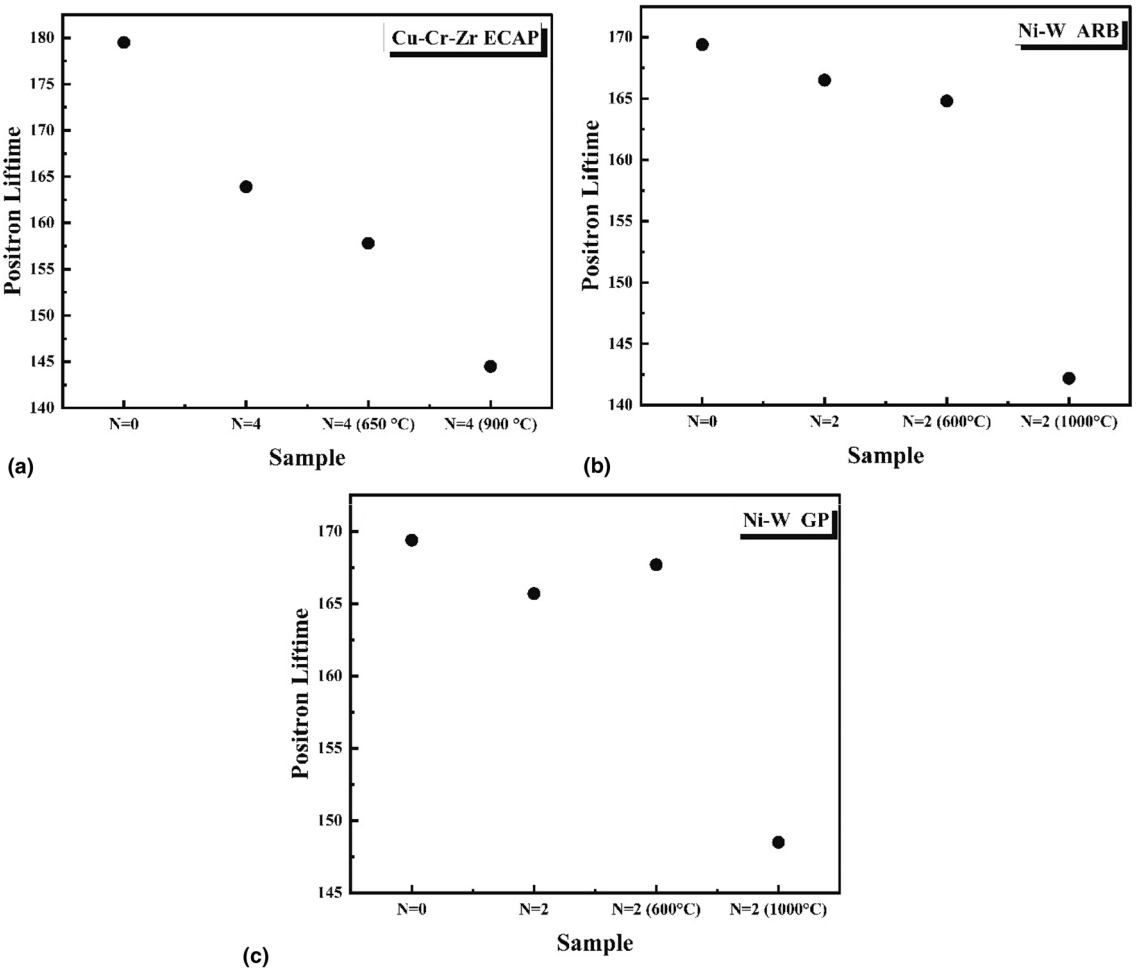

Figure 2. Evolution of the lifetime τ_1 of the (a) Cu–1Cr–0.1Zr (wt%) alloy after ECAP processing and aging and (b) Ni–14W (wt%) alloy after ARB processing up to 2 cycles and (c) after GP processing up to 2 cycles and aging.

in the range of several ps only and therefore a precise and definitive defect identification is excluded.

After annealing at 900°C for 1 h, τ_1 drops seriously to a value close to 144.5 ps (I_1 = 62.6%). This drop may be associated with a complete recrystallization and rapid grain growth as already observed in cold rolled and annealed pure Cu.[32]

It is worth noting that even after annealing at 900°C for 1 h, τ_1 value is larger than bulk life time of Cu matrix. This may be explained by the presence of residual and stable defects such as defect-solute or defect-precipitates complexes.[32] Indeed, Cu–Cr–Zr is an age-hardenable alloy and many authors reported about the nature and sequence of different Cu_xZr_y precipitates that can appear (besides Cr clusters) after annealing conventional or severe plastic deformation of Cu–Cr–Zr alloy.[40,41]

In the literature, a PALS analysis after cold rolling and recrystallization annealing and grain growth at 250–850°C temperatures of a Cu–Ni–Si alloy showed that this alloy behaves very differently from pure copper.[32] Indeed, annealing pure copper causes a decrease of the positron lifetime that is explained by a phenomenon of recovery-recrystallization which annihilates. In the case of Cu–Ni–Si, more complicated behavior was observed. The average life time of the positrons increases up to 184 ps indicating an obvious formation of large vacancy clusters.[30] This is not in line with the present finding where τ_1 lifetime got decreasing continuously which plaids against a possible the on existence of vacancy clusters in Cu–Cr–Zr alloy samples after ECAP processing.

Figure 2(b), (c) show the variation of positron lifetime τ_1 as a function of the thermo-mechanical processing of the Ni–14%W alloy after severe plastic deformation by ARB and GP and annealing respectively. Quite small decrease (169 to 166 ps) of τ_1 values between the initial state (N = 0) and the deformed state after two-cycle either by ARB or GP while the intensity increased from 65 to 69%. A subsequent annealing at 600° C for 1 h is accompanied by a versatile decrease of τ_1 and I_1 after ARB (τ_1 = 164.8 ps, I_1 = 65.9%) processing while it increased after GP processing (τ_1 = 167.8 ps, I_1 = 70.8%).

In the literature, it is reported that positron bulk life time for Ni ranges between 111 and 116 ps and the trapped positron lifetime at single vacancy is around 147–180 ps while in dislocations it is around 150 ps.[42] Following Čížek et al.,[38] the statement "positron trapped at dislocation" will mean the process involving temporally trapping of a positron in the dislocation line and its final annihilation in a point defect associated with the dislocation. Moreover, it is generally accepted that positrons trapped at a dislocation line diffuse quickly along the line and are eventually trapped at point defects associated with the dislocation as a vacancy bound to dislocation or jog at dislocation.[43–45]

In the work of Yuasa et al.,[26] the positron lifetime ascribed to positron annihilation at one-atom-sized (or smaller) vacancies, at vacancy clusters, and at nanosized voids were in the ranges $\tau_1 \sim 150$–200 ps, $\tau_2 \sim 400$–450 ps and $\tau_3 \sim 2000$–2500 ps, respectively. Indubitably, even if the electrodeposition technique is suitable to produce nanomaterials with reduced internal flaws, non- negligible amounts of dislocations can be introduced during the deposition procedure.[46] Therefore, in the author's opinion, the shorter lifetime τ_1 should correctly be associated with vacancy bound to dislocation. The range values of τ_2 let suggest the presence of vacancy clusters in Ni–W alloy after SPD processing and annealing but the present values of τ_2 has a mean value slightly below the lower limit of the 400–450 ps corresponding to the trapping at vacancy clusters. However, cautiously, one cannot exclude their presence. Indeed, Yuasa et al.[26] reported a relative intensity τ_2/τ_1 in the ratio 1/8. In the present work, very plausibly, one can speculate that vacancy cluster contribution to the annihilation is somewhat convoluted with the source contribution.

A noticeable drop of τ_1 down to ($\tau_1 = 142.2$ ps, $I_1 = 63.6\%$) and ($\tau_1 = 148.5$ ps, $I_1 = 65.2\%$) is evidenced after annealing at 1000°C the Ni–W alloy samples after ARB and GP, respectively. This drop is very probably due to the recrystallization phenomenon and grain growth concomitant to reduction in dislocation density via a relaxation process and thus reduces the lifetime of the positrons. The τ_1 and I_1 values after GP processing and annealing are manifestly higher than those after ARB. This fact should be expected since the GP processing generates less dislocation amount in the material than ARB processing[2] and therefore leads to longer positron lifetime.

Globally, a surprising similar evolution of τ_1 after severe plastic deformation by GP and annealing is noticed. This implies that the annihilation processes material are almost unchanged during plastic deformations (ARB and GP) vis-à-vis the sensitivity of the positrons to the generated defects.

Figure 3 show the Vickers microhardness of Cu–Cr–Zr and Ni–W alloys in different thermomechanical states. For Cu–Cr–Zr alloy, the hardness in the homogenized state was about 80 Hv. It seemed to increase up to 100% after severe plastic deformation by ECAP after 4 passes. Annealing treatment at 400 and 650°C temperatures for 1 h does not seem to affect the achieved value. On the other hand, annealing treatment at 900°C for 1 h softens the material to reach a value of the hardness close to that of the homogenized state. This decrease is a natural softening due to the recrystallization process that occurs in the material during annealing at 900°C. Almost the same trends are observed for Ni–W alloy. Only a slight evolution of the hardness is depicted after GP and annealing where the fluctuations did not exceed 5% of the initial value [Fig. 3(b)]. This modest hardening of the Ni–W alloy during GP processing has been already observed and discussed by Koriche et al.[2] Indeed, these authors claimed that the modest hardening is explained by an absence of strong grain refinement that should enhance the hardness when it is concomitant with an increase of dislocation density. However, the evolution was stronger after ARB processing (~45% of the initial value). Fundamentally, the evolution of the hardness do corroborate the positron annihilation lifetime spectroscopy results presented in [Fig. 3(a)–(c)].

A good correspondence between the hardness and lifetime evolution has been evidenced in pure Cu after cold-rolling and annealing.[21] This accordance was not so longer valid for Cu–Ni–Si alloy as it is in pure Cu.[21] The inconsistency suggested an extra-effect of the precipitation on the evolution of the

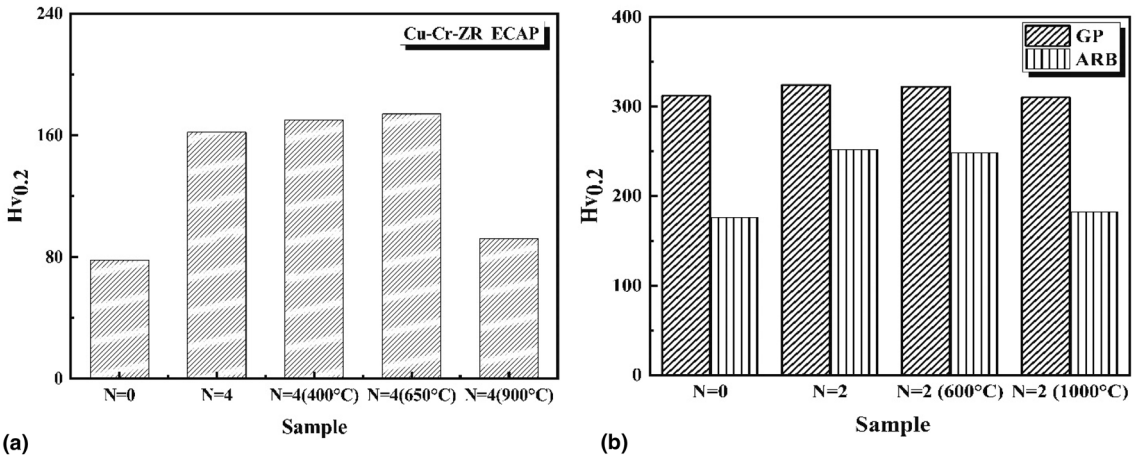

Figure 3. Microhardness evolution of: (a) Cu–Cr–ZR alloy ECAP processing up to 4 passes and annealing and (b) Ni–14W alloy after ARB and GP processing up to 4 cycles and annealing.

hardness. Indeed, it is well known that the precipitate responsible for the strengthening effect in Cu–Ni–Si is the δ-Ni2Si phase. It is quite surprising that the Cu–Cr–Zr alloy shows a good hardness/lifetime correspondence even if a precipitation of Cr clusters and Cu_3Zr phase occur in this system upon annealing. But this may be explained by the fact the effect of precipitates phases in Cu–Cr–Zr is not so huge (< 30% hardness gain[47,48]) than in Cu–Ni–Si (< 160% hardness gain[21]).

Conclusion

Based on the present results of a positron annihilation lifetime spectroscopy (PALS) and microhardness measurements, following conclusions have been drawn:

- Almost all the PALS spectra bear the same trends. The spectra were a sum of three exponential decay components.
- The dominant τ_1 component, which corresponds to positrons trapped at vacancies bound to dislocation shows significant changes. It slightly decreases after SPD processing comparatively to the as received state.
- The PALS analysis did not evidence any lifetime associated with vacancy cluster or microvoids.
- After annealing at high temperature, τ_1 seriously. This drop may be associated with a recovery of the prevailing vacancy clusters and is indicative of rapid grain growth and complete recrystallization.
- τ_1 value is larger than bulk life time of Cu and Ni matrix. This may be explained by the presence of residual and stable defects such as defect-solute or defect-precipitates complexes.
- The Ni–W alloy samples behave similarly during plastic deformations (ARB and GP) and annealing vis-à-vis the sensitivity of the positrons to the generated defects in the material.
- The evolution of the microhardness correlate well with the positron annihilation lifetime spectroscopy results. A net softening due to recrystallization, grain growth and relaxation of the defect structure is evidenced after annealing high temperature namely 900 and 1000°C for Cu–Cr–Zr and Ni–W alloys respectively.
- The thermal evolution of the UFG structure (determined by PALS and hardness measurements) is quite similar in UFG Cu–Cr–Zr and Ni–W alloys processed by ECAP and ARB/GP, respectively.

Acknowledgments

The authors wish to thank Dr. Y. ATEBA BETANDA from APERAM alloys, France and Dr. T. BAUDIN from ICMMO, University Paris-Saclay, France, for kindly providing the Ni–W alloy and help.

Funding

This work was supported in part the international PHC-MAGHREB Program N° 16MAG03.

Declarations

Competing interests

The authors declare that they have no known competing financial interests or personal relationships that could have appeared to influence the work reported in this paper.

References

1. V. Subramanya Sarma, J. Eickemeyer, L. Schultz, B. Holzapfel, Recrystallisation texture and magnetisation behaviour of some FCC Ni-W alloys. Scr. Mater. **50**, 953–957 (2004). https://doi.org/10.1016/j.scriptamat.2004.01.004
2. S. Koriche, S. Boudekhani-Abbas, H. Azzeddine, K. Abib, A.L. Helbert, F. Brisset, T. Baudin, D. Bradai, On the groove pressing of Ni-W alloy: microstructure, texture and mechanical properties evolution. Kovove Mater. **56**, 313–323 (2018). https://doi.org/10.4149/km_2018_5_313
3. D.J. Edwards, B.N. Singh, S. Tähtinen, Effect of heat treatments on precipitate microstructure and mechanical properties of a CuCrZr alloy. J. Nucl. Mater. **367**, 904–909 (2007). https://doi.org/10.1016/j.jnucmat.2007.03.064
4. H. Fuxiang, M. Jusheng, N. Honglong, G. Zhiting, Analysis of phases in a Cu–Cr–Zr alloy. Scr. Mater. **48**, 97–102 (2003). https://doi.org/10.1016/S1359-6462(02)00353-6
5. Z.Q. Wang, Y.B. Zhong, X.J. Rao, C. Wang, J. Wang, Z.G. Zhang, W.L. Ren, Z.M. Ren, Electrical and mechanical properties of Cu-Cr-Zr alloy aged under imposed direct continuous current. Trans. Nonferr. Met. Soc. **22**, 1106–1111 (2012). https://doi.org/10.1016/S1003-6326(11)61290-9
6. K. Abib, F. Hadj-Larbi, L. Rabahi, B. Alili, D. Bradai, DSC analysis of commercial Cu-Cr-Zr alloy processed by equal channel angular pressing. Trans. Nonferr. Met. Soc. **25**, 838–843 (2015). https://doi.org/10.1016/S1003-6326(15)63671-8
7. K. Abib, J.A.M. Balanos, B. Alili, D. Bradai, On the microstructure and texture of Cu-Cr-Zr alloy after severe plastic deformation by ECAP. Mater. Charact. **112**, 252–258 (2016). https://doi.org/10.1016/j.matchar.2015.12.026
8. T.G. Langdon, Twenty-five years of ultrafine-grained materials: achieving exceptional properties through grain refinement. Acta Mater. **61**, 7035–7059 (2013). https://doi.org/10.1016/j.actamat.2013.08.018
9. R.Z. Valiev, Y. Estrin, Z. Horita, Producing bulk ultrafine-grained materials by severe plastic deformation: ten years later. JOM. **68**, 1216–1226 (2016). https://doi.org/10.1007/s11837-016-1820-6
10. Y. Saito, N. Tsuji, H. Utsunomiya, S. Tanigawa, R.G. Hong, Ultra-fine grained bulk steel produced by accumulative roll-bonding (ARB) process. Scr. Mater. **40**, 795–800 (1999). https://doi.org/10.1016/S1359-6462(99)00015-9
11. R.Z. Valiev, I.V. Alexandrov, Y.T. Zhu, T.C. Lowe, Paradox on of strength and ductility in metals processed by SPD. J. Mater. Res. **17**, 5–8 (2002). https://doi.org/10.1557/JMR.2002.0002
12. W. Habila, H. Azzeddine, B. Mehdi, K. Tirsatine, T. Baudin, A.L. Helbert, F. Brisset, S. Gautrot, M.H. Mathon, D. Bradai, Investigation of microstructure and texture evolution of a Mg/Al laminated composite elaborated by accumulative roll bonding. Mater. Charact. **147**, 242–252 (2019). https://doi.org/10.1016/j.matchar.2018.11.010
13. K. Tirsatine, H. Azzeddine, T. Baudin, A.L. Helbert, F. Brisset, B. Alili, D. Bradai, Texture and microstructure evolution of Fe-Ni alloy after accumulative roll bonding. J. Alloys Compd. **610**, 352–360 (2014). https://doi.org/10.1016/j.jallcom.2014.04.173
14. A.K. Gupta, T.S. Maddukuri, S.K. Singh, Constrained groove pressing for sheet metal processing. Prog. Mater. Sci. **84**, 403–462 (2016). https://doi.org/10.1016/j.pmatsci.2016.09.008

15. R.Z. Valiev, R.K. Islamgaliev, I.V. Alexandrov, Bulk nanostructured materials from severe plastic deformation. Prog. Mater. Sci. **45**, 103–189 (2000). https://doi.org/10.1016/S0079-6425(99)00007-9
16. M. Zehetbauer, R.Z. Valiev, *Nanomaterials by Severe Plastic Deformation* (Wiley-VCH, Weinheim, 2004), pp.21–46
17. J. Čížek, I. Procházka, B. Smola, I. Stulíková, R. Kužel, M. Cieslar, Z. Matěj, V. Cherkaska, G. Brauer, W. Anwand, R.K. Islamgaliev, O.B. Kulyasova, Positron annihilation studies of microstructure of ultra fine grained metals prepared by severe plastic deformation. Mat. Sci. Forum. **482**, 207–210 (2005). https://doi.org/10.4028/www.scientific.net/msf.482.207
18. A. Dupasquier, A.P. Mills Jr., *Positron Spectroscopy of Solids* (IOS Press, Amsterdam, 1995), pp.14–18
19. J. Gubicza, in *Defect Structure in Nanomaterials*, ed. by J. Gubicza (Woodhead Publishing, 2012), pp. 41–83
20. J. Čížek, M. Janeček, O. Srba, R. Kužel, Z. Barnovská, I. Procházka, S. Dobatkin, Evolution of defects in copper deformed by high-pressure torsion. Acta Mater. **59**, 2322–2329 (2011). https://doi.org/10.1016/j.actamat.2010.12.028
21. J. Čížek, I. Procházka, R. Kužel, Z. Matej, V. Cherkaska, M. Cieslar, B. Smola, I. Stulikova, G. Brauer, W. Anwand, R.K. Islamgaliev, O. Kulyasova, Ultra fine-grained metals prepared by severe plastic deformation: a positron annihilation study. Acta Phys. Pol. A **107**, 745–752 (2005). https://doi.org/10.12693/APhysPolA.107.745
22. J. Čížek, O. Melikhova, Z. Barnovská, I. Procházka, R.K. Islamgaliev, Vacancy clusters in ultra fine grained metals prepared by severe plastic deformation. J. Phys. Conf. Ser. **443**, 012008 (2013). https://doi.org/10.1088/1742-6596/443/1/012008
23. P.V. Kuznetsov, A.M. Lider, Yu.S. Bordulev, R.S. Laptev, T.V. Rakhmatulina, A.V. Korznikov, Grain-subgrain structure and vacancy-type defects in submicrocrystalline nickel at low temperature annealing. Acta Phys. Pol. A **128**, 714–718 (2015). https://doi.org/10.12693/APhysPolA.128.714
24. S.V. Divinski, J. Ribbe, D. Baither, G. Schmitz, G. Reglitz, H. Rösner, K. Sato, Y. Estrin, G. Wilde, Nano- and micro-scale free volume in ultrafine grained Cu–1wt%Pb alloy deformed by equal channel angular pressing. Acta Mater. **57**, 5706–5717 (2009). https://doi.org/10.1016/j.actamat.2009.07.066
25. R. Würschum, W. Greiner, H.E. Schaefer, Preparation and positron lifetime spectroscopy of nanocrystalline metals. Nanostruct. Mater. **2**, 55–62 (1993). https://doi.org/10.1016/0965-9773(93)90050-L
26. M. Yuasa, H. Matsumoto, M. Hakamada, M. Mabuchi, Effects of vacancies on deformation behavior in nanocrystalline nickel. Mater. Trans. **49**, 2315–2321 (2008). https://doi.org/10.2320/matertrans.MRA2008115
27. S. Van Petegem, F. DallaTorre, D. Segers, H. Van Swygenhoven, Free volume in nanostructured Ni. Scripta Mater. **48**, 17–22 (2003). https://doi.org/10.1016/S1359-6462(02)00322-6
28. V. Slugen, J. Kuriplach, P. Ballo, P. Domonkos, G. Kögel, P. Sperr, W. Egger, W. Triftshäuser, V.M. Domankova, P. Kovac, I. Vavra, S. Stancek, M. Petriska, A. Zeman, Positron annihilation investigations of defects in copper alloys selected for Nuclear Fusion Technology. Fusion Eng. Des. **70**, 141–153 (2004). https://doi.org/10.1016/j.fusengdes.2003.10.002
29. V. Slugen, P. Domonkoš, Advanced positron annihilation studies of CuCrZr alloys. J. Nucl. Mater. **557**, 153164 (2021). https://doi.org/10.4028/www.scientific.net/msf.255-257.233
30. A. Shukla, L. Hoffmann, A.A. Manuel, M. Peter, Melt 40 a program for positron lifetime analysis. Mat. Sci. Forum. **255**, 233–237 (1997). https://doi.org/10.4028/www.scientific.net/msf.255-257.233
31. Z. Lounis-Mokrani, A. Guittoum, D. Imatoukene, M. Aitziane, A. Badreddine, M. Mebhah, Characterisation of proton irradiated CR-39 detector using positron annihilation lifetime spectroscopy. Radiat. Meas. **50**, 26–30 (2013). https://doi.org/10.1016/j.radmeas.2012.10.007
32. N. Qi, Y.L. Jia, H.Q. Liu, D.Q. Yi, Z.Q. Chen, The evolution of defects in deformed Cu-Ni-Si alloys during isochornoal annealing stuied by positron annihilation. Chin. Phys. Lett. **29**, 12107803-1-4 (2012). https://doi.org/10.1088/0256-307X/29/12/127803
33. J. Čížek, I. Procházka, M. Cieslar, R. Kužel, J. Kuriplach, F. Chmelık, I. Stulıková, F. Becvar, O. Melikhova, Thermal stability of ultrafine grained copper. Phys. Rev. B **65**, 094106 (2002). https://doi.org/10.1103/PhysRevB.65.094106
34. F. Bečvář, J. Cížek, I. Procházka, Use of energy summing for selection of coincidence events in positron-lifetime spectroscopy. Acta Phys. Pol. A **95**, 448–454 (1999). https://doi.org/10.12693/APhysPolA.95.448
35. A.P. de Lima, C. Lopes Gil, D.R. Martins, N. Ayres de Campos, L.F. Menezes, J.V. Fernandes, in *Proceedings of the European Meeting on Positron Studies of Defects*, vol. 2, part 1, ed. by G. Dlubek, O. Brümmer, G. Brauer, K. Hennig (Martin-Luther-Universität Halle-Wittenberg, Wernigerode, 1987), p. C1
36. R. Würschum, W. Greiner, R.Z. Valley, M. Rapp, W. Sigle, O. Schneeweiss, H.-E. Schaefer, Interfacial free volumes in ultra-fine grained metals prepared by severe plastic deformation, by spark erosion, or by crystallization of amorphous alloys. Scripta Met. **25**, 2451–2456 (1991). https://doi.org/10.1016/0956-716X(91)90048-6
37. N.M. Nancheva, On the possibility of the positron annihilation method to detect vacancy clusters in shock-loaded metals. J. Mech. Work. Technol. **15**, 215–227 (1987). https://doi.org/10.1016/0378-3804(87)90035-0
38. J. Čížek, I. Procházka, M. Cieslar, I. Stulíková, F. Chmelík, R.K. Islamgaliev, Positron-lifetime investigation of thermal stability of ultra-fine grained nickel. Phys. Status Solidi A **191**, 391–408 (2002). https://doi.org/10.1002/1521-396X(200206)191:2%3c391::AID-PSSA391%3e3.0.CO;2-H
39. M. Hatakeyama, T. Toyama, J. Yang, Y. Nagai, M. Hasegawa, T. Ohkubo, M. Eldrup, B.N. Singh, 3D-AP and positron annihilation study of precipitation behavior in Cu-Cr-Zr alloy. J. Nucl. Mater. **386–388**, 852–855 (2009). https://doi.org/10.1016/j.jnucmat.2008.12.266
40. A. Vinogradov, V. Patlan, Y. Suzuki, K. Kitagawa, V.I. Kopylov, Structure and properties of ultra-fine grain Cu-Cr-Zr alloy produced by equal-channel angular pressing. Acta Mater. **50**, 1639–1651 (2002). https://doi.org/10.1016/S1359-6454(01)00437-2
41. J.H. Su, P. Liu, Q.M. Dong, H.J. Li, F.Z. Ren, B.H. Tian, Recrystallization and precipitation behavior of Cu-Cr-Zr alloy. J. Mater. Eng. Perform. **16**, 490–493 (2007). https://doi.org/10.1007/s11665-007-9071-x
42. J.M. Campillo Robles, F. Plazaola, Collection of data on positron lifetimes and vacancy formation energies of the elements of the periodic table. Defect Diffus. Forum. **213**, 141–236 (2003). https://doi.org/10.4028/www.scientific.net/ddf.213-215.141
43. L.C. Smedskjaert, M. Manninen, M.J. Flusst, An alternative interpretation of positron annihilation in dislocations. J. Phys. F: Met. Phys. **10**, 2237–2249 (1980). https://doi.org/10.1088/0305-4608/10/10/019
44. Y.K. Park, J.T. Waber, M. Meshii, C.L. Snead, C.G. Park, Dislocation studies on deformed single crystals of high-purity iron using positron annihilation: determination of dislocation densities. Phys. Rev. B **34**, 823–836 (1986). https://doi.org/10.1103/PhysRevB.34.823
45. J. Čížek, I. Procházka, T. Kmječ, P. Vostrý, Using of modified trapping model in positron-lifetime study of cold-worked aluminum. Phys. Status Solidi A **180**, 439–458 (2000). https://doi.org/10.1002/1521-396X(200008)180:2%3c439::AID-PSSA439%3e3.0.CO;2-9
46. T. Ungár, A. Révész, A. Borbély, Dislocations and grain size in electrodeposited nanocrystalline Ni determined by the modified Williamson-Hall and Warren-Averbach procedures. J. Appl. Crystallogr. **31**, 554–558 (1998). https://doi.org/10.1107/S0021889897019559
47. K. Abib, H. Azzeddine, K. Tirsatine, T. Baudin, A.L. Helbert, F. Brisset, B. Alili, D. Bradai, Thermal stability of Cu-Cr-Zr alloy processed by equal-channel angular pressing. Mater. Charact. **118**, 527–534 (2016). https://doi.org/10.1016/j.matchar.2016.07.006
48. K. Abib, H. Azzeddine, B. Alili, L. Lityńska-Dobrzyńska, A.L. Helbert, T. Baudin, P. Jegou, M.H. Mathon, P. Zieba, D. Bradai, Cr cluster characterization in Cu-Cr-Zr alloy after ECAP processing and aging using SANS and HAADF-STEM. Kovove Mater. **57**, 121–129 (2019). https://doi.org/10.4149/km_2019_1_121